© Universiti Tun Hussein Onn Malaysia Publisher's Office

IJIE

Journal homepage: http://penerbit.uthm.edu.my/ojs/index.php/ijie
ISSN : 2229-838X e-ISSN : 2600-7916

The International Journal of Integrated Engineering

Broken Insulator Effects on Charge Distribution Measurement along Suspension Insulators

H. Rosli[1], N. A. Othman [1]*, M. A. M. Piah[2], N. A. M. Jamail[1], M. F. M. Yousof[1], M. N. Ismail[1]

[1]Department of Electrical Power Engineering, Faculty of Electrical and Electronic Engineering, Universiti Tun Hussein Onn Malaysia (UTHM), 86400 Batu Pahat, Johor, MALAYSIA

[2]School of Electrical Engineering, Faculty of Engineering, Universiti Teknologi Malaysia (UTM), 81310 Johor Bahru, Johor, MALAYSIA

*Corresponding Author

DOI: https://doi.org/10.30880/ijie.2020.12.02.012
Received 29 December 2019; Accepted 27 January 2020; Available online 28 February 2020

Abstract: In the early years of power system network, porcelain and glass were used and still continuously serve the overhead lines to the present time. Obviously, they can provide distinction services over a long period of time. In spite of that, one or two of the insulators in the suspension may be damaged due to some cases yet the suspension insulator is believed can still be used for a certain amount of time. By studying some research from previous works, it is accepted that the different properties of porcelain and glass type had made these insulators vary in their respective capabilities to serve overhead lines. This paper endeavours the distribution of charge for the porcelain suspension insulator using chamber method. Finite element software particularly Quickfield™ was used in simulation purpose to validate the experimental results. Similar patterns of charge distributions were acquired for both experimental and simulation works.

Keywords: Space charge, transmission line, porcelain insulators, broken insulators, finite element software

1. Introduction

It is accepted fact that high voltage (HV) insulators located in transmission line towers serve to prevent any unwanted current flow. These insulators are devices used to separate and support electrical conductors in the overhead line as illustrated in Fig. 1. It is known that the transmission lines carry high power from generator, hence the need of insulators that can withstand very high voltage stresses is 97mportant (Sims, 2013). Thus, overhead transmission insulators are agreed of having an important role as significant as other equipment in the overhead line. They are also partly dependent by the transmission network. Besides the insulation, the insulators also gives mechanical support between transmission lines and the towers (Ahmad, 1986)(Othman *et al.*, 2014). Studies on insulator strings were reported since 1920s by researchers named Ryan and Henline which pioneered to many publications since then (Durand, 1934)(Denholm, 1960)(R. Bonzano, M. Ricca, E. Garbagnati, G. Marrone, 1991). In 1979, an investigator published about safety concerns on broken units to conductive live line maintenance (Throop, 1979). The voltage distribution of broken suspension insulators is still continuously studied to date, in fact have received wide attention from researchers worldwide.

Generally, insulators can be categorized into two types i.e. ceramic type which consists of glass and porcelain, and polymeric type. Despite the pros on each types of insulators on the transmission lines for their services, once they happen to have physical impacts, it may lead to the failure of the insulator itself. The common factors of the insulation failures

*Corresponding author: ndiana@uthm.edu.my

includes radial cracking, corrosion of pin, and brittle fractures (Maciej, Lucas and Daniel, 2005). But it is important to note that the failure modes of the insulators are entirely different from each other.

Fig. 1 - Transmission line tower structure in UTHM

This paper will be discussed on ceramic insulator focusing on porcelain type. In the presence of external breakdown, glass insulators may result in completely broken whilst porcelain insulator can be broken in chunk and leaves large remaining pieces of sheds. It can be assumed that the remaining large pieces of porcelain in suspension insulator can still serve the transmission line even though in partially condition. Thus, this paper proposed to study about the space charge distribution on the broken porcelain insulator when the broken unit is included in the suspension insulator. Furthermore, many researchers had studied about the space charge behaviour in dielectric materials using various methods (Andoand Numajiri, 1979)(Khalil and Hansen, 1988)(Ieda, 1990)(Ono, Nakazawa and Oda, 2004).

Understanding that the insulation material may be the reason of space charge accumulation in solid dielectric, the importance of space charge phenomena has resulted in considerable efforts to develop the space charge measurement techniques. For this reason, quite a few efforts have been made during the last decades to develop non-destructive techniques of space charge measurement as attempts to improve the destructive techniques invented years before. Such measurements open the way to understand the processes taking place in the dielectric under the study, and make it possible to select materials and interfaces which minimized the risks of breakdown in HV applications (Bamji and Bulinski, 2001)(Collins, 1975).

Typically, space charge proliferation in insulation is categorized into homocharge and heterocharge according to respective polarity of charge and the adjacent electrode as shown in Fig. 2. Referring to **Error! Reference source not found.**, heterocharge relates to the charge with the diverse polarity to the adjacent electrode and vice versa (Xu, 2009). According to the researcher, during the injection near electrode, the charges have low mobility moving across the insulator material hence the homocharge. Homocharge will then releases the electric field stress of the insulator surface and thusly increases the stress in the insulator material.

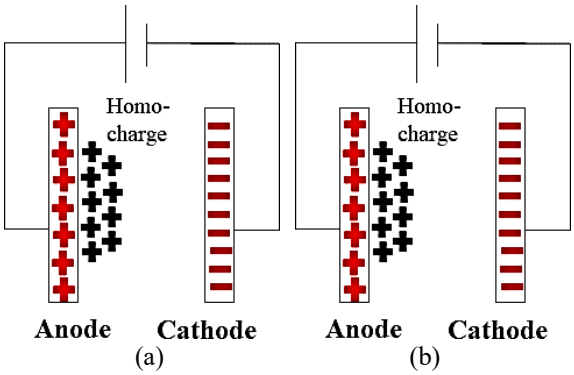

Fig. 2 - The concept of homocharge and heterocharge

Meanwhile, heterocharge happens if the insulator material transport charges facilely than they extracted by the surface. As the ion mobility is perceptible, the ion will move to the opposite polarity electrode of the applied stress. Hence, the increasing of electric stress of the insulator surface and release the stress in the insulator material.

The imbalance charge rate may be caused by electric field due to the moving or trapped charges. The prior operations are considered in the formation of space charge in the insulating material under electric field can be delineated according to (Lewiner, 1986).

Firstly, the electric field in homogenous material acquaint the dipole charge inside the insulation bulk and the space charge happens near both electrodes. Next, the ions moved due to the electric field. The positive charges moved towards negative charges and vice versa. Building on that, the positive charges accumulate in bulk near GND whilst negative charges accumulate near HV electrode. This situation is basically referred as heterocharge. Furthermore, the space charge formation can be triggered also by the charge generated at electrodes. This type is commonly referred as homocharge that will happen near the electrode with the same polarity.

Space charge can occur within dielectrics that are stressed by high electric fields. Trapped space charge within solid dielectrics are often a contributing factor leading to dielectric failure within HV power cables and capacitors. Consequently, the space charge effect on insulators is important to understanding and the damage affecting the distribution system should be investigated. Hence, this study is to investigate the space charge distribution on broken porcelain suspension insulator.

2. Materials and Methods

In order to obtain the space charge distribution results, an experimental setup depicted in Fig. 3 has been employed based on an electrostatic kit from Vernier Software and Technology (Othman et al., 2014). The tested insulators were experimented in a chamber box made of acrylic sheet with measuring size of 50 cm x 50cm x 80 cm (width x length x height). The acrylic sheet was chosen mainly because of the highest transparency which can ease the process of observation throughout the experiment.

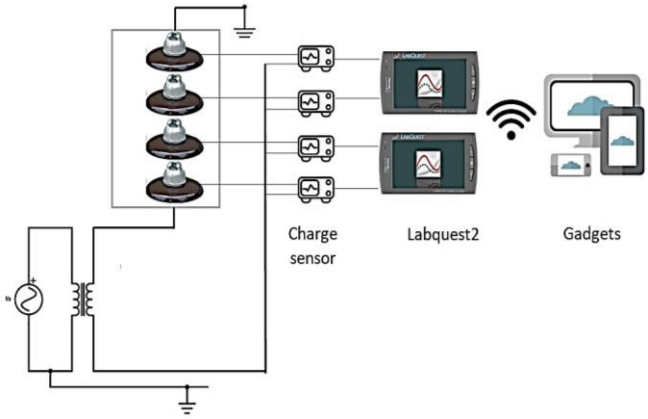

Fig. 3 - Experimental setup

The setup was concerned with the standard operating procedures (SOP) for the benefits of the person performing the experiment and the audiences as well. The pictorial view of experimental setup conducted in the laboratory is shown in Error! Reference source not found.. In this setup, a radially shaped mesh made of galvanized steel was attached surrounding the string insulators. Each mesh was then connected to four units of charge sensors (CS) for data collection. Throughout this experiment, the insulators were applied with 33 kV AC voltage at 50 Hz in the duration of 30 minutes.

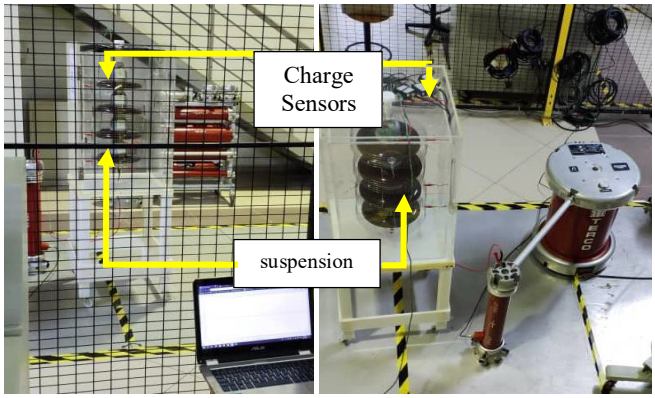

Fig. 4 - Experimental setup of space charge measurement on porcelain insulator

The insulators hanged in the chamber were successfully applied practically of 33 kV on it without any breakdown occurred. The initial observation that can be seen during the testing was the mesh surrounding the string insulators is vibrated in a very small movement but enough to set eyes on. Concurrently, it was recorded from the control desk that the current pertained was 1.2A. Rationally, the vibrating of the mesh can be considered as the respond from current flows across the string insulators. The CS and Labquest2 were placed on top of the chamber to capture the space charge distribution data. Four units of CS were used to capture the charge distribution on four unit of insulators as detailed in **Error! Reference source not found.**. The CS was paired with respective insulators and transmit the collected data to Labquest2. Via Wi-Fi, the results displayed on Labquest2 were monitored using a laptop.

Table 1 - The pair of CS and insulators in the chamber

Charge Sensor (CS)	Insulator
CS1	Insulator 1 (I1)
CS2	Insulator 2 (I2)
CS3	Insulator 3 (I3)
CS4	Insulator 4 (I4)

To validate the space charge distribution data obtained from the experimental works, a simulation modelling using finite element software was performed. Four units of cap and pin type porcelain insulators particularly model type ANSI 52-3 was used as the sample to be tested. The insulator was miniature in a free space using Quickfield^{TM} Professional software for the simulation purpose. The technical parameters of the porcelain insulator are presented in **Error! Reference source not found.**.

Table 2 - Technical parameters of the simulated porcelain insulator

Types of material	Relative Electric Permittivity (Ω·m)
Cement	2
Steel	1000
Porcelain	6.0
Air	1

It is worth mentioning that AC stress of 33 kV was applied to the 4th insulator (nearest to HV electrode) pin of porcelain insulator and the 1st insulator (top insulator cap) was grounded. Since the insulator has a symmetrical shape, this simulation process was performed in an axisymmetric 2D model class. The cross-sectional area of porcelain insulator is presented in Fig. 5.

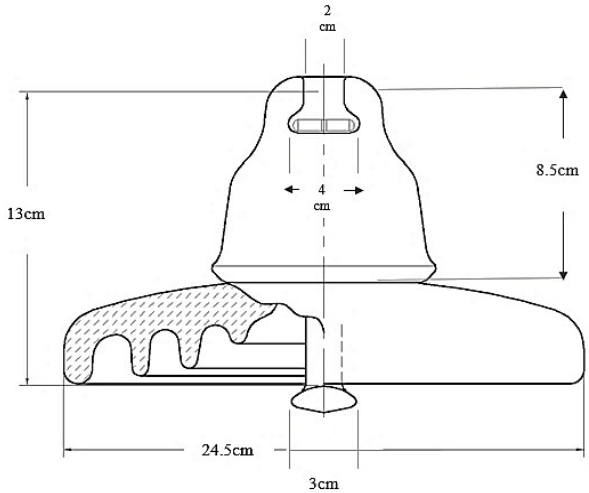

Fig. 5 - The cross-sectional diagram of porcelain insulator

In order to analyse the broken porcelain insulator on space charge distribution subjected to dissimilarity of the broken insulator in the suspension insulator, four configurations were simulated. Each configuration was assigned as tabulated in **Error! Reference source not found.** where the location of the broken porcelain insulator for each case is in different position.

Table 3 - The location of broken configuration in suspension insulator

String with 4 units of porcelain insulators	Designation
No broken porcelain insulator present	000
Broken porcelain insulator located in the top, 1st position (near GND)	100-1
Broken porcelain insulator located in the 2nd position (upper middle)	100-2
Broken porcelain insulator located in the 3rd position (lower middle)	100-3
Broken porcelain insulator located in the lowest, 4th position (near HV)	100-4

A pictorial of the configuration of perfect insulator string is shown in Fig. 6.

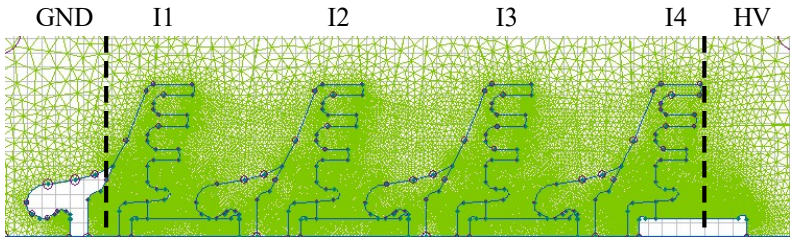

Fig. 6 - Perfect insulator string modelled in Quickfield™

3. Results and Discussion

The primary purpose of this section is to explain and discuss all results extracted from the conducted simulation and experimental works in order to meet the objective mentioned earlier. The discussion is sorted by focusing on experimental works of perfect suspension insulator followed by simulation works of perfect suspension insulator, and finally comparing with the broken insulator effects on charge distribution measurement along the suspension insulators.

3.1 Experimental Outcome of Charge Distributions

Fig. 7 shows the space charge distribution porcelain insulator surface with different broken cases. The recorded results show different amplitude of charge distribution for all the broken cases. According to Neagu and Dias (Neagu and Dias, 2009), the process of injection and extraction occurred at the HV electrode and GND terminal affects the variability of the charge distribution. The injection process is believed initiating the electrons migrate to the next insulator through the atmosphere at a very slow rate to the middle part of the suspension insulator (I2 & I3). Thus, the charge distribution in the middle part have more negative charges.

It is noticed that highest amplitude of positive charge was found at I1 especially in the perfect suspension insulator and when the broken insulator was located near to HV electrode. The accumulation of positive charge in AC stress can be considered as crucial especially when it became more dominant since it can cause the degradation process of insulation material (Chong *et al.*, 2006)(Fukuma, 2001).

Meanwhile, for the broken cases on both upper and lower middle of suspension insulator (100-2 and 100-3), the amplitudes of charge are slightly decreased compared to the perfect suspension insulator. However, when the broken insulator was located near to HV electrode (100-4), it can be observed that the amplitude of the charge distribution on I4 is the highest compared to other insulators.

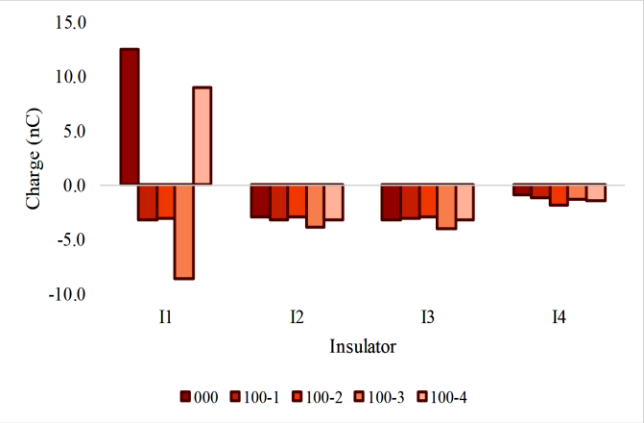

Fig. 7 - Experimental results of charge distribution on suspension porcelain insulator

3.2 Simulation Outcome of Charge Distribution

The distribution of space charge extracted from the simulation works is presented in Fig. 8. It is obvious that the charge distribution from simulation works when broken insulator happened in the suspension insulator are tend to be negative distributed. Similarly, as in the experimental results, the voltage injection occurred at HV electrode causing slow migration electrons to the GND across the insulators. Also, the extraction at GND terminal affect charge distribution on I1. Moreover, electric field is also one of the factors that give consequence dependence of space charge in solid insulators (Kumada and Okabe, 2004)(Othman *et al.*, 2017)(McAllister, Crichton and Pedersen, 1994)(Davies and Chen, 1992).

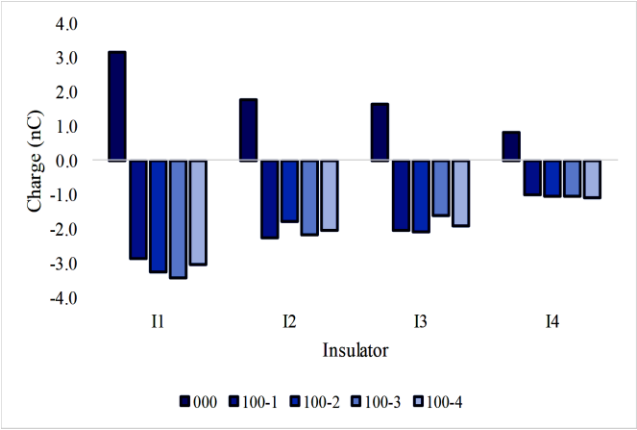

Fig. 8 - Simulation results of charge distribution on suspension insulator

It is believed that some electrons emanate from the high field electrode may become negative ions, while others may remain as electrons when traversing the space gap. As reported in (Zhou *et al.*, 2007), the generated positive charges is very little accumulated near to electrode due to insufficient period to drive the ions into the dielectrics when positive pulse was injected. However, the negative pulse can drive electrons to reach dielectrics directly proportional.

3.3 Comparison of Experimental and Simulation Outcome

Fig. 9 compares the results obtained from simulation and experimental works for charge distribution on perfect suspension insulator. Experimentally, it is important to highlight that the charge distribution recorded were the average of positive and negative charge combined altogether. It is apparent from Fig. 9 that I4 and I1 collected the highest and the lowest charge distribution, respectively. This condition can be explained by considering that the voltage injection applied on I4 initiated the electron to move to the next insulator. Accepting the fact that electron move faster and easily than positive charge, the charge amplitude is observed to be increasing from I4 to I1. It is best to understand that when the insulator is near to the source, the charge distribution pattern can be considered as homocharge (Chen, Chong and Fu, 2006).

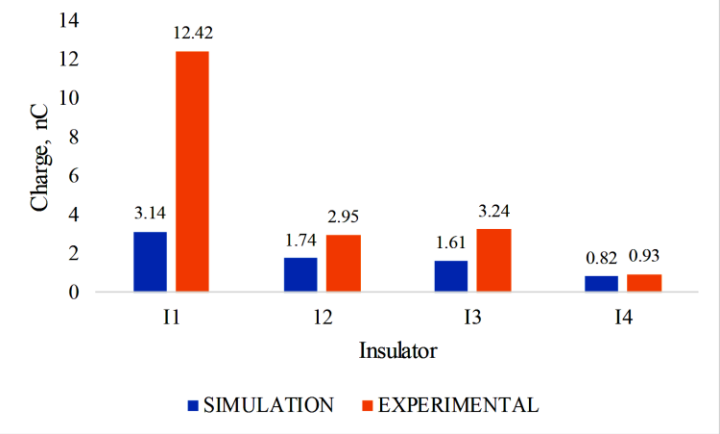

Fig. 9 - Space charge average on perfect suspension insulator

Fig. 10 compares the results from experimental and simulation works for space charge distribution on broken suspension insulator. There is no argument that the charge distributed on all of the insulators increases when broken insulator was included in the suspension insulator. Based on a previous study, the accumulation of space charge may lead to the electric field distortion which eventually causing the breakdown of insulation (Salah, 1997). According to the observation on Fig. 10 (b) and Fig. 10 (c), when broken insulator happened in the middle part of the suspension insulator, the highest charge amplitude is recorded on I1. Knowing that the space charge drift under the action of the electric field, the insulator near to the GND terminal is affected (Rosli *et al.*, 2017). This statement is proven in this case where the charge distribution is the most affected at GND when broken insulators are located in I2 and I3.

The charge amplitude reaches the highest at GND when the broken insulator is located in the lower middle of suspension insulator (I3). The injected charge carriers move across the dielectrics under the influence of electric field.

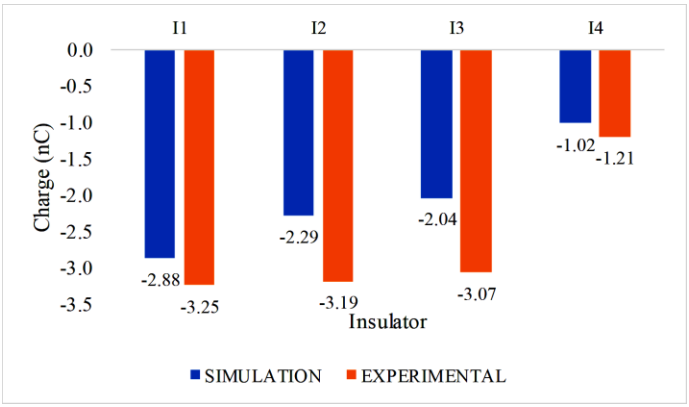

(a)

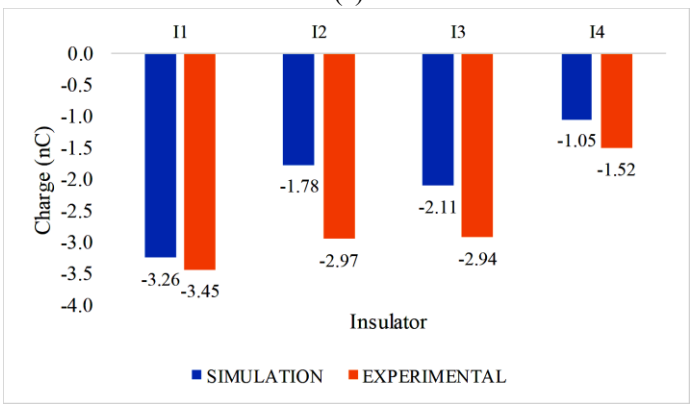

(b)

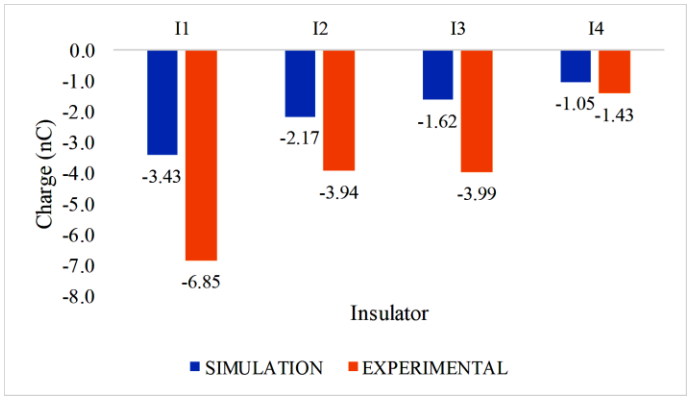

(c)

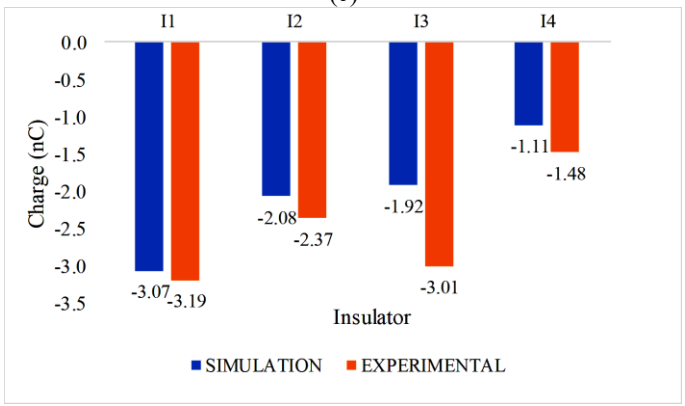

(d)

Fig. 10 - Space charge average on broken suspension insulator, (a) near GND (100-1); (b) at upper middle (100-2); (c) at lower middle (100-3); and (d) near HV (100-4)

4. Conclusion

This paper conducted an investigation on the influence of broken porcelain insulator on charge distribution measurement along suspension insulators. The results are completed with assorted conclusions. The data collected from experimental and simulation both established the similar pattern of charge distribution across the suspension insulators for all configurations. Furthermore, it is proven that the charge amplitude in GND terminal reached the maximal when the broken insulator is located in the middle of the suspension insulator. Equivalently, the authors believe the effect of charge distribution on broken insulator also is due the distortion of electric field.

Acknowledgement

The authors would like to thank the Geran Penyelidikan TIER 1 2017 (U863) and Geran Penyelidikan Pasca Siswazah GPPS (U948), Office for Research Innovation, Commercialization and Consultancy Management (ORICC) and Registrar of Universiti Tun Hussein Onn Malaysia (UTHM) who was supported the research paper.

References

[1] Ahmad, H. B. (1986). Effects of Topology, Environmental Conditions and Damped Oscillatory Surges on the Performance of Suspension Insulator Strings.
[2] Ando, N. and Numajiri, F. (1979). Experimental investigation of space charge in xlpe cable using dust figure, IEEE Transactions on Electrical Insulation, EI-14(1), 36-42.
[3] Bamji, S. S. and Bulinski, A. T. (2001). Luminescence in polymeric insulation and its implication on insulation aging, 453-458.
[4] Chen, G., Chong, Y. L. and Fu, M. (2006). Calibration of the pulsed electroacoustic technique in the presence of trapped charge, Measurement Science and Technology, 17(7), 1974-1980.
[5] Chong, Y. L. et al. (2006). Space charge and charge trapping characteristics of cross-linked polyethylene subjected to ac electric stresses, Journal of Physics D: Applied Physics, 39, 1658-1666.
[6] Collins, R. E. (1975). Distribution of charge in electrets, Applied Physics Letters, 26(12), 675-677.

[7] Davies, A. E. and Chen, G. (1992). Electric stress distribution in polymeric insulation containing defect sites and space charge, COMPEL - The International Journal for Computation and Mathematics in Electrical and Electronic Engineering, 11(1), 237-240.
[8] Denholm, A. S. (1960). Electric stress grading of insulator strings, (August), p. 647.
[9] Durand, W. F. (1934) 'Harris joseph ryan 1866-1934', XIX.
[10] Fukuma, M. (2001). Space charge dynamics in ldpe films immediately before breakdown, IEEE Transactions on Dielectrics and Electrical Insulation, 8(2), 2001-2003.
[11] Ieda, M. (1990). Study of space charge effects in polyethylene by thermal-pulse current techniques, 25(3), 509-514.
[12] Khalil, M. S. and Hansen, B. S. (1988). Investigation of Space Charge in Low-Density Polyethylene Using a Field Probe Technique, IEEE Transactions on Electrical Insulation, 23(3), 441-445.
[13] Kumada, A. and Okabe, S. (2004). Charge distribution measurement on a truncated cone spacer under dc voltage, IEEE Transactions on Dielectrics and Electrical Insulation, 11(6), 929-937.
[14] Lewiner, J. (1986). Evolution of experimental techniques for the study of the electrical properties of insulating materials, IEEE Transactions on Electrical Insulation, EI-21(3), 351-360.
[15] Maciej, K., Lucas, K. and Daniel, A. (2005). Failure analyses of nonceramic insulators Part 1: Brittle fracture characteristics, IEEE Electrical Insulation Magazine, 21(3), 14-27.
[16] McAllister, I. W., Crichton, G. C. and Pedersen, A. (1994). Charge accumulation in dc cables: a macroscopic approach, Conference Record of the 1994 IEEE International Symposium on Electrical Insulation, Pittsburgh, PA USA, 212-216.
[17] Neagu, E. R. and Dias, C. J. (2009). Charge injection/extraction at a metal-dielectric interface: Experimental validation - [Feature article], IEEE Electrical Insulation Magazine, 25(1), pp. 15-22.
[18] Ono, R., Nakazawa, M. and Oda, T. (2004). Charge storage in corona-charged polypropylene films analyzed by LIPP and TSC methods, Industry Applications, IEEE Transactions on, 40(6), 1482-1488.
[19] Othman, N. A. et al. (2014). Characterization of charge distribution on the high voltage glass insulator string, Journal of Electrostatics. Elsevier Ltd, 72(4), 315-321.
[20] Othman, N. A. et al. (2017). Space charge distribution and leakage current pulses for contaminated glass insulator strings in power transmission lines, 11, 876-882.
[21] R. Bonzano, M. Ricca, E. Garbagnati, G. Marrone, A. P. (1991). Experimental research on the behaviour of hv cap and pin insulator strings with failed units, European Transactions on Electrical Power, European Transactions on Electrical Power, 37-46.
[22] Rosli, H. et al. (2017). Potential and electric field characteristics of broken porcelain insulator, International Journal of Electrical and Computer Engineering, 7(6), 3114-3123.
[23] Salah, M. (1997). International research and development trends and problems, IEEE Electrical Insulation Magazine, 13(6), pp. 35-47.
[24] Sims, S. (2013). High-voltage overhead transmission lines (HVOTLs) and house prices, Towers, Turbines and Transmission Lines: Impacts on Property Value, 45-53.
[25] Throop, R. S. (1979). Safety aspects of changing broken and punctured suspension insulators using live-line methods.
[26] Xu, Z. (2009). Space charge measurement and analysis in low density polyethylene films.
[27] Zhou, Y. X. et al. (2007). Nanosecond pulse corona charging of polymers, IEEE Transactions on Dielectrics and Electrical Insulation, 14(2), 495-501.